
Boom clay drying behavior : experimental and numerical study

J. Hubert^{1,4}, E. Plougonven², N. Prime³, A. Leonard², F. Collin¹

¹ Department ArGEnCo, University of Liège, Belgium

² Dpt. Chimie appliquée, University of Liège, Belgium

³ Dpt. University Savoie Mont-Blanc LOCIE, France

⁴ FRS-FNRS, Fonds National de la Recherche Scientifique

RÉSUMÉ. Ce papier présente le modèle utilisé pour simuler le séchage de l'argile de Boom. Une campagne expérimentale a été menée à bien [PRI 16] et ses résultats sont utilisés afin de valider le modèle utilisé. La première partie de ce papier est donc consacrée à un bref rappel de la campagne expérimentale. Ensuite, les différentes équations et paramètres du modèle utilisé sont détaillés. Finalement, des simulations numériques sont effectuées et permettent de mettre en exergue la capacité dudit modèle à représenter précisément le comportement observé expérimentalement.

ABSTRACT. This paper presents a thermo-hydro-mechanical model for simulating the drying behavior of Boom Clay. The experimental campaign conducted by Prime et al [PRI 16] is briefly presented since it will be used to validate the model. Then, the different sub-models are introduced and finally, numerical simulations were performed to illustrate the capability of the proposed model to reproduce the observed behavior.

MOTS-CLÉS : Milieu poreux, Séchage convectif, Transfer de masse et de chaleur, retrait

KEYWORDS: Porous medium, Convective drying, Mass and heat transfer, Shrinkage

1. Introduction

Nuclear power plants are an efficient way of producing energy but they are also generating long-lived high activity radioactive wastes. Therefore, a problem remains : what to do with the nuclear waste ?

They are hazardous to both environment and human health and, thus, need to be isolated from the biosphere until their radioactivity decays enough to not pose a threat. For that reason, they are subjected to very restrictive regulations by national agencies (In Belgium, isolation procedure are based on a waste classification established by ONDRAF (Organisme National des Déchets Radioactifs et des matières Fissiles enrichies) in collaboration with the European Commission has established [Bel 13]). The scientific community is thus faced with the task of finding technical solutions to respect those regulations. The long term management of high activity waste is internationally studied and the envisioned solution is deep geological storage [NEA 08]. The geological layer needs to have a very low permeability [IEA 03] to seal the wastes safely and permanently so that it should never pose a threat to the environment.

1.1. Concept of the deep geological storage

The waste isolation is guaranteed by the combination of engineered and natural barriers referred to as the multi-barrier principle. The solution chosen for the engineered barrier in Belgium, is presented Figure 1 [CRA 09] :

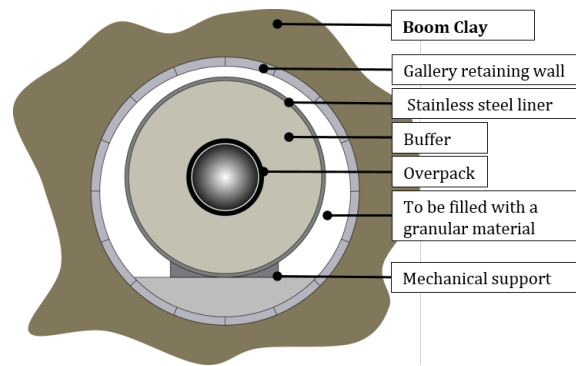


Figure 1. Multi-barriers principle

The super-containers are placed within galleries over 200m deep . These galleries are then backfilled with a granular material (a mix of sand and bentonite is considered) which is used to prevent any collapse of the gallery, provide a good enough geochemical environment and present a thermal conductivity high enough to allow the heat transfer.

1.2. Scope of the study

Within that framework, in Belgium, Boom Clay is considered [BER 07] as an host formation for deep geological storage. It presents very low water conductivity and a high radionuclides retention capacity. Those properties make it a good candidate for nuclear waste storage. An Underground Research Facility (URF) has been built in the north of the country, near Mol, to study the feasibility of deep geological disposal.

Given the importance of insuring good sealing conditions for nuclear waste storage, the potential host rock - Boom Clay - response to the many stresses induced by the excavation of the galleries and the storage of high activity waste is thoroughly studied. Specifically, its drying behavior is still relatively unexplored and a good understanding of the coupled thermo-hydro-mechanical processes occurring between the host rock and the ventilation air is required to go a step further toward a better management of our nuclear wastes. Indeed, the ventilation needed to allow for people circulation during the construction and operation phase could induce a desaturation of the host rock. That dessication can, in turn, lead to cracking and thus to the loss of the sealing properties.

1.3. Introduction to the drying kinetics

To be able to study the drying behavior of Boom Clay, one need to understand how to analyze the porous medium - atmosphere interaction. These interactions have long been studied through experiments using either

saline solutions or convective dryers. The latter allow to reproduce natural drying conditions and the analysis of the results gives us a better understanding of the multi-physics processes occurring at the porous medium surface. This analysis is made in the framework of the boundary layer model (see section 3.1).

The drying kinetics of samples can be analyzed based on weight measurements during the drying process. Three curves can be used to study the drying kinetics : the mass loss evolution with the drying time (Figure 2), the drying rate evolution with time (Figure 3) and the drying rate evolution with water content (Figure 4). The latter is constructed based on the formers and is called Krischer's curve.

Krischer's curve is used because it gives more clear and complete indications about the drying kinetics of materials [LÉO 02b]. On this curve, three periods can be observed [IDS 74] :

- I : Preheating Period
- II : Constant Rate Period (CRP)
- III : Falling Rate Period (FRP)

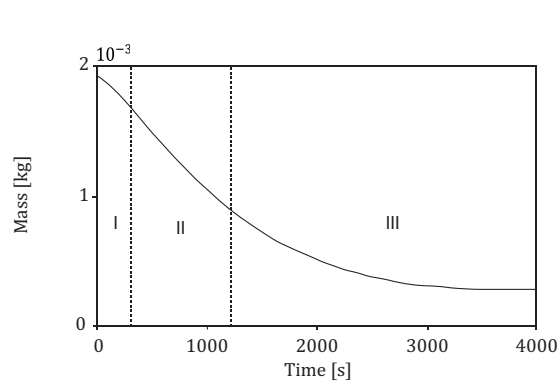


Figure 2. Mass loss with time

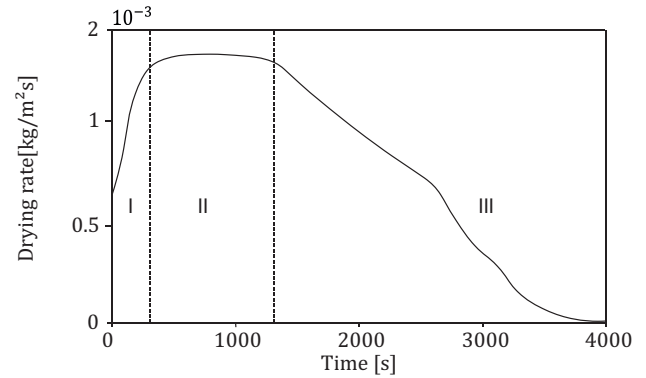


Figure 3. Drying rate evolution with time

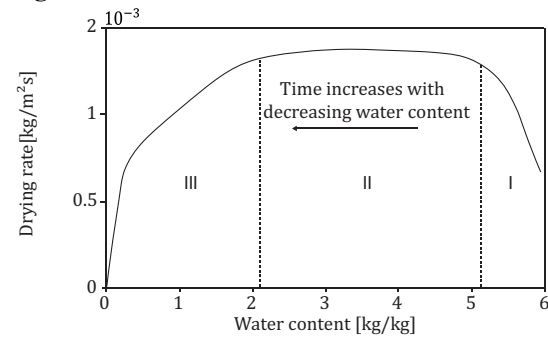


Figure 4. Krischer's curve

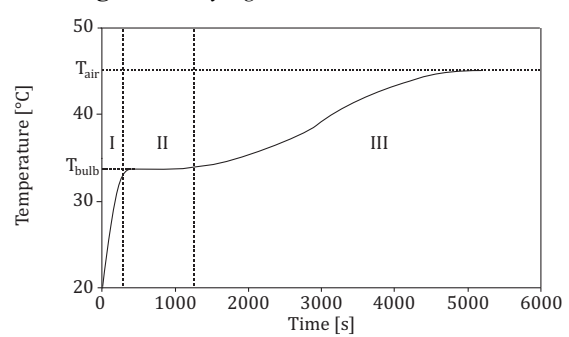


Figure 5. Temperature evolution with time

Krischer's curve is studied in parallel with the evolution of the temperature with time (Figure 5). This is the behavior observed in the case where the drying air temperature is significantly higher than the sample initial temperature [GER 10]. This was also measured experimentally by Musielak and Jacek [MUS 07].

Preheating period

It is very short and corresponds to an increase in drying rate. The temperature at the surface of the sample also increases from its initial value to the temperature of the wet bulb [GER 10].

Constant Rate Period (CRP)

The CRP appears at the beginning of the drying process. It is characterized by a constant drying rate. The heat supply is completely used for the evaporation of the liquid water at the surface of the sample and thus, the

temperature remains constant and equal to the temperature of the wet bulb. The evaporation occurs in a saturated boundary layer. The vapor and the heat transfers are only influenced by the external conditions, i.e. the drying temperature or the air velocity [NAD 95]. This period will last until the sample is no longer saturated and internal transfers start to influence the drying rate.

Falling Rate Period (FRP)

It is characterized by an increase in the dried body temperature from the wet bulb temperature to the drying fluid temperature. The drying rate decreases because of the decrease in permeability with the desaturation of the medium.

1.4. Layout of the paper

This paper aims at explaining clearly the drying behavior of Boom clay. To do so, an experimental campaign was conducted [PRI 16]. Its protocol and results will be briefly presented in section 2. However, this paper will put emphasis on the numerical modeling of the problem. It will be shown in section 5 that the suggested model is capable of closely reproducing the behavior observed experimentally. This paper is closed by section 6 with a few final remarks.

2. Experimental campaign

Convective drying tests were performed on Boom Clay samples. The experiments are briefly described from the samples preparation to the data acquisition and the obtained results. More details about experiments are available in Prime *et al* [PRI 16].

2.1. Studied material

Boom Clay is a rock formation located beneath the Mol-Dessel nuclear zone (north-east of Belgium). It is interesting because of its properties making it one of the formation potentially suitable for deep geological nuclear waste disposal [OND 01].

It has been the subject of numerous experimental studies since more than 30 years, such as Bernier *et al* [BER 07], Chen *et al* [CHE 11], Dehandschutter *et al* [DEH 05], Horseman *et al* [HOR 87], etc. They were mainly aimed at characterizing the geological and geotechnical properties of Boom Clay to better understand its thermo-hydro-mechanical behavior. Based on the results obtained by those studies in the last decades, Boom Clay is considered as a plastic clay, moderately over-consolidated. Wemaere *et al* and Blümling *et al* [WEM 08, BLÜ 07] have shown that Boom Clay presents a strong anisotropy induced by the clay structure (horizontal bedding with alternance of clayey and silt materials). The thermo-hydro-mechanical properties of Boom Clay are well documented already and a good compilation of it can be found in the work of Dizier [DIZ 11].

2.2. Samples preparation

Several cylindrical samples were water drilled from the cores received from the Mol laboratory. Those samples were of around 35 mm of diameter and 35 mm of height. The drilling was made so that the bedding direction would be parallel to the cylinder axis to allow for a faster saturation process. Other smaller samples were taken from the core sample to determine the water retention curve of the material.

The samples were then placed into a triaxial cell to saturate them under *in situ* conditions. Since the saturation is a time consuming process, it was necessary to optimize the use of the saturated samples to perform as many drying tests as possible for repeatability reasons. The saturated samples were, thus, divided into smaller cylinders of respective height of 5, 10 and 15 mm. Those smaller cylinders were then cut in four quarters from which a 15 mm diameter cylinder is extracted.

Those samples are weighed and dipped into a warm paraffin bath and then into a colder one. The warm bath was necessary to ensure good adherence between paraffin and samples and the colder one to get a paraffin layer thick enough to ensure efficient sealing. The finished products were stored into a desiccator saturated with water. The whole process was done as quickly as possible and the samples were carried in a desiccator partly filled with water to prevent any drying.

2.3. Drying test

The test were made using a micro convective dryer designed in the Laboratory of Chemical Engineering of the University of Liège [LEO 02a]). It is suited for drying light samples using a convective air flow with controlled temperature and velocity. Twelves small samples were tested. They were named using the following method : the sample height in millimeters followed by the sample number (example : 5-1 for the first 5 mm height sample).

The paraffin on the top surface was removed to dry them from the top surface only. They were submitted to a convective air flow with a velocity of 0.8 m/s , a temperature of 25°C and with a relative humidity of around 3.5%. The air flow was kept as parallel as possible to the drying surface to reproduce as closely as possible *in situ* conditions. Those conditions are quite harsh and lead to intense drying.

3. Thermo-hydraulic model

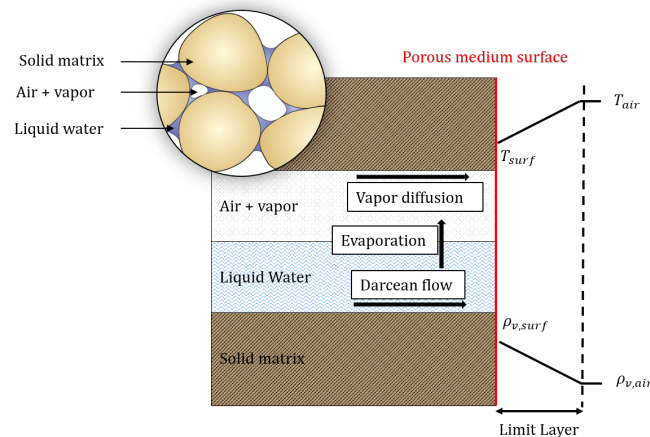


Figure 6. Water transfer mechanism

Boom Clay is considered to be an unsaturated porous medium with a solid phase, a liquid and gas phase as shown at Figure 6. Within that medium, the liquid water transfers are governed by Darcy's equation and vapor diffusion is controlled by Fick's law. Evaporation at the surface of the medium and heat transfer are calculated using the boundary layer model.

3.1. Vapor and heat exchange

The results are analyzed based on the assumption of the existence of a boundary layer all around the sample where the mass and heat transfers are assumed to take place [KOW 12]. The water flow, \bar{q} , from the materials to the surroundings is assumed to be proportional to the difference between the vapor density of the drying fluid, $\rho_{v,air} [kg/m^3]$, and at the surface of the sample, $\rho_{v,surf} [kg/m^3]$, [GER 08, LÉO 05]. The proportionality coefficient is a mass transfer coefficient, $\alpha [m/s]$, characterizing the surface transfer properties. The water flow is expressed as :

$$\bar{q} = \alpha(\rho_{v,surf} - \rho_{v,air}) \quad (1)$$

The heat flux, \bar{f} , from the boundary to the drying air is expressed as :

$$\bar{f} = L\bar{q} - \beta(T_{air} - T_{surf}) \quad (2)$$

where $T_{air} [^\circ\text{C}]$ is the temperature of the drying air, $T_{surf} [^\circ\text{C}]$ is the temperature at the surface of the sample, β is a heat transfer coefficient and L is water evaporation latent heat (2500 kJ/kg).

Based on the drying kinetics, it is possible to determine the transfer coefficients (Eq. 1 and Eq. 2). The value of the drying rate during the CRP is directly linked to capacity of the drying air to evaporate the water at the surface

of the porous medium and is thus linked to the value of the mass transfer coefficient. Hence, to determine the value of the transfer coefficient, the value of the drying rate during the CRP is used. Same can be said of the heat transfer, the drying rate used is the one during the CRP and during that period, the temperature corresponds to the wet bulb temperature which can be analytically determined. So no measurements of the temperature are actually required and only knowing the drying rate is sufficient to determine the heat transfer coefficient. The mean mass and heat transfer coefficients are around respectively 0.048 [m/s] and 53.5 [W/m/K] with a standard deviation inferior to 10% for all the samples tested.

3.2. Internal transfers

The clay is an unsaturated porous medium, partly saturated by liquid water and gas (air + vapor). The water mass balance equation is based on Richard's equation :

$$\underbrace{\frac{\partial(\rho_w n S_{r,w})}{\partial t} + \text{div}(\rho_w \underline{f}_w)}_{\text{Liquid Water}} + \underbrace{\frac{\partial(\rho_v n S_{r,g})}{\partial t} + \text{div}(\underline{i}_v + \rho_v \underline{f}_g)}_{\text{Water Vapor}} = Q \quad (3)$$

where ρ_w [kg/m³] and ρ_v [kg/m³] are respectively the water and the vapor densities, n [-] is the porosity, $S_{r,w}$ [-] and $S_{r,g}$ [-] are respectively the water and the gas saturation degrees in volume, t [s] the time, Q [kg/s] is the injected flux, \underline{f}_w [m/s] and \underline{f}_g [m/s] are the water and gas phase respective macroscopic velocity and \underline{i}_v [kg/m²s] is the non-advective flux of water vapor.

Liquid water flow

Liquid water macroscopic velocity is given by the generalization of Darcy's law :

$$\underline{f}_w = - \frac{k_{rel}(S_{r,w}) \underline{k}_{sat}}{\mu_w} (\nabla p_w + g \rho_w \nabla z) \quad (4)$$

in which, k_{rel} [-] is the relative permeability, \underline{k}_{sat} [m²] the intrinsic saturated permeability, p_w [kPa] the water pressure, g [m/s²] the gravity acceleration, μ_w [kg/m/s] the water viscosity and z [m] is the upwards vertical spatial coordinates. The relative permeability k_{rel} can be determined based on degree of saturation and the formulation proposed by van Genuchten :

$$k_{rel} = \sqrt{S_{r,w}} \left(1 - \left(1 - S_{r,w}^{\frac{1}{m_{vG}}} \right)^{m_{vG}} \right)^2 \quad (5)$$

where m_{vG} [-] is a model parameter. The retention curve links the water saturation as a function of the capillary pressure. The formulation proposed by van Genuchten [VAN 80] is used in our model :

$$S_{r,w} = S_{res} + (S_{sat} - S_{res}) \left(1 + \left(\frac{p_c}{\alpha_{vG}} \right)^{n_{vG}} \right)^{-m_{vG}} \quad (6)$$

in which n_{vG} [-], m_{vG} [-] are model parameters, α_{vG} [kPa] is a model parameter related to the air entry pressure, S_{res} [-] is the residual water saturation, S_{sat} [-] is the maximal water saturation and p_c [kPa] is the capillary pressure.

Anisotropic intrinsic permeability

The advective flow of water depends on the anisotropy of the material considered. This is taken into account by introducing an anisotropic intrinsic permeability tensor. However, most materials present limited forms of anisotropy and stratified materials require only two parameters for the description of the water flow and in the case of vertical layering, only vertical and horizontal hydraulic permeability are needed.

Vapor diffusion

The water vapor flow is assumed to follow a Fick's diffusion law in a tortuous medium. The vapor diffusion is linked to gradient of vapor density :

$$\underline{i}_v = -D_{atm} \tau_v n S_{r,v} \nabla(\rho_v) \quad (7)$$

where D_{atm} [m²/s] molecular diffusion coefficient and τ_v [-] is the tortuosity. Vapor is assumed to be in equilibrium with liquid water.

3.3. Heat diffusion

To be able to simulate the temperature evolution within the medium, we use the classic governing energy balance equation :

$$\dot{S}_T + \text{div}(V_T) - Q = 0 \quad (8)$$

where \dot{S}_T is the heat storage, V_T is the heat flux and Q is the heat production term. In the derived balance equation 8, the heat storage term can be expressed as follows :

$$S_T = nS_{w,r}\rho_w c_{p,w}(T-T_0) + nS_{a,\rho_a}c_{p,a}(T-T_0) + (1-n)\rho_s c_{p,s}(T-T_0) + nS_{r,g}\rho_v c_{p,v}(T-T_0) + nS_{r,g}\rho_v L \quad (9)$$

in which, $c_{p,w}$, $c_{p,a}$, $c_{p,s}$ are respectively the water, the air and the solid specific heats [J/kgK], ρ_w , ρ_a , ρ_s are respectively the water, the air and the solid densities [kg/m^3]. The heat flux consists of a conduction term proportional to the thermal conductivity of the porous medium and a convective term related to the heat transported by fluid flows :

$$V_T = -\Gamma\nabla T + c_{p,w}\rho_w \underline{f}_w(T-T_0) + c_{p,a}\rho_a \underline{f}_g(T-T_0) + c_{v,a}(\rho_v \underline{f}_g + \underline{i}_v)(T-T_0) + (\rho_v \underline{f}_g + \underline{i}_v)L \quad (10)$$

where Γ [W/mK] is the porous medium thermal conductivity, T_0 is the initial temperature and T is the temperature.

4. Mechanical model

Given the anisotropy of the material studied, the mechanical model chosen is an orthotropic elastic model. Elasticity is allowed since after elasto-plastic simulations, no plasticity was observed in the range of stresses reached during the drying test.

Bishop's effective stress has been chosen to describe the stress-strain relation because it directly incorporates the effect of the suction. It is expressed as :

$$\sigma'_{ij} = \sigma_{ij} - p_g \delta_{ij} + S_{r,w}(p_g - p_w)\delta_{ij} \quad (11)$$

where σ'_{ij} [kPa] is the effective stress tensor, σ_{ij} [kPa] is the total stress tensor, $S_{r,w}$ [-] is the water saturation and δ_{ij} is Kronecker's tensor. p_g and p_w denote respectively gas and water pressure [kPa].

The strain is related to the effective stress through the following relation :

$$\sigma'_{ij} = D_{ijkl}^e \epsilon_{ij} \quad (12)$$

where σ'_{ij} is the elastic stress tensor and ϵ_{ij} is the elastic strain and D_{ijkl}^e is Hooke's tensor.

5. Experimental and Numerical Results

From the recurrent weighing of the samples, the drying kinetics can be determined. The shrinkage profile and evolution is obtained using the evolution of the cross sections surface measured with the microtomography. For the sake of simplicity, only the results exploited in this paper are presented. The results presented below are those obtained for sample 5-1 which was arbitrarily chosen. This is acceptable because as seen in Prime *et al* [PRI 16] there is very little dispersion in the results from one sample to another and their behavior is very similar. All other results and more detailed analysis are available in Prime *et al* [PRI 16].

At the same time, the model introduced in section 3 - 4 is used to represent the drying behavior of the Boom clay samples dried during the experimental campaign.

Drying kinetics

The mass evolution with time is presented at Figure 7 and shows that the dry state is reached after a bit more than 20h with intense drying during the first 2 or 3 hours of the test. The drying rate can be calculated based on the mass loss and the evaporation surface :

$$q = -\frac{1}{S} \frac{dm}{dt} \quad (13)$$

where m [g] and S [m^2] are respectively the measured mass and cross section of the sample.

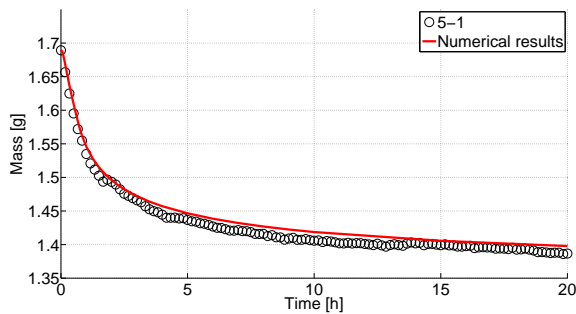


Figure 7. Comparison of experimental and numerical mass loss for sample 5-1

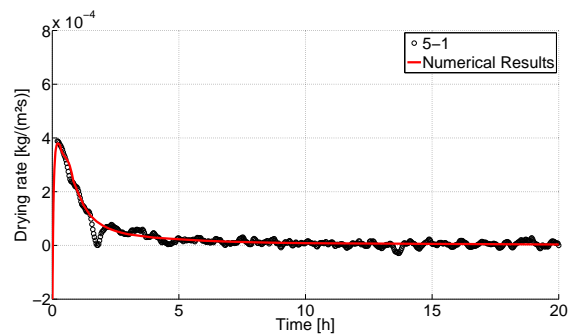


Figure 8. Comparison of experimental and numerical drying rate evolution with time for sample 5-1

Since clay undergoes shrinkage during the drying, the actualized surface is used to compute the drying rate. This surface is obtained through the microtomography measurement. The evolution of the drying rate with time and Krischer's curve can thus be expressed as shown respectively at Figure 8 and Figure 9. The rough curves exhibit heavy fluctuations which are due to the small time step between two weighing during which mass may not vary enough. Consequently, the curves have been smoothed with Lanczos filter [LAN 88].

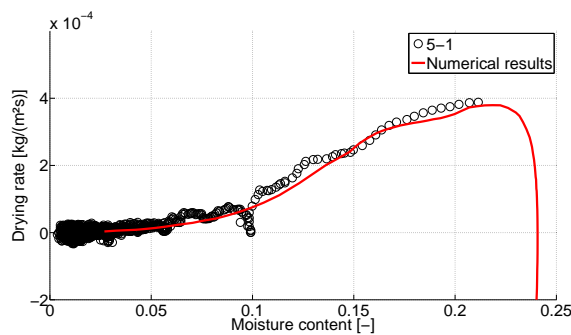


Figure 9. Comparison of experimental and numerical Krischer's curve for sample 5-1

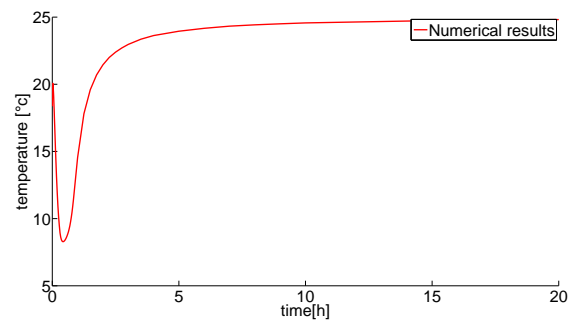


Figure 10. Numerical variation of the temperature with time at the drying surface

Contrary to the theoretical curve, there is little to no CRP observable. This is due to Boom clay very low water permeability which is "slowing down" the water trying to reach the surface of the sample. Thus the drying rate is limited by the capacity of the water to reach the evaporating surface rather than by the capacity of the drying fluid to evaporate the water at the surface of the sample. Internal transfers are limiting the drying from the beginning of the drying test. The variation in the slope of the drying rate is linked to the desaturation of the sample and the decrease in permeability coming with it as explained in section 1.3. Moreover, the water contents seems to be continuous showing no significant moisture loss occurs during the scanning.

Figure 7, Figure 8 and Figure 9 all show good fitting of the experimental results confirming the ability of the suggested model to represent the drying behavior of porous unsaturated material. Specifically, the model is able to represent the behavior of very low permeability materials despite the numerical problems inherent to the calculation of water flows in low permeability materials.

Temperature

Since the temperature of the sample was not recorded during the drying test, no validation of the experimental results is possible. Nonetheless, the numerical results are presented at Figure 10. The temperature decreases from its initial value of 17°C (temperature of the room) to a minimum around 8°C. This is logical since the drying air temperature (25°C) is not very high and therefore, the heat provided by the drying air is not sufficient to enable the evaporation on its own. Heat from the porous medium is thus used and the temperature of the sample decreases until it reaches the temperature of the wet bulb. No constant value period is observed since we do not have any

CRP. When the drying rate decreases, the evaporation process is less intense and the heat supply is more than the quantity needed for the evaporation and so the temperature of the sample increases until it reaches the temperature of the drying air.

Shrinkage

Using the micro-tomography, images of the cross section of the sample are obtained. The analysis of those images returns the surface of the sample cross section. The ratio between this value and the initial surface of that same cross section gives the relative shrinkage. On Figure 11, most of the shrinkage takes place at the very beginning of the drying (around 2/3 of the final strain has developed after 1 hour). Numerical result on Figure 11 is a little less accurate at the beginning but the final shrinkage of the sample is very similar in both cases.

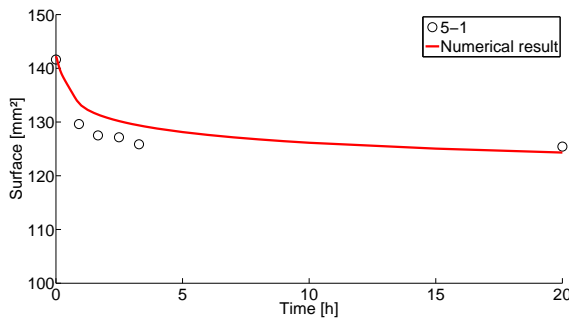


Figure 11. Comparison of experimental and numerical shrinkage profile with time

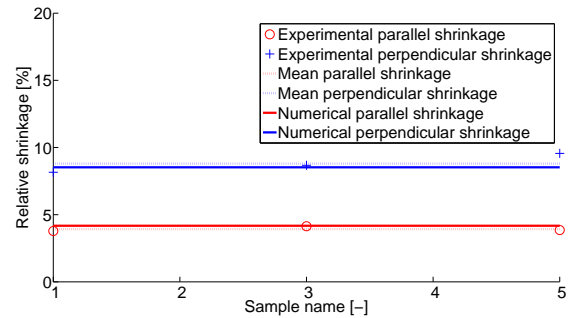


Figure 12. Comparison between numerical and experimental shrinkage values for all the samples tested

Figure 12 shows the final shrinkage in the direction parallel and normal to the bedding direction of all the samples tested. The dotted lines are the mean values and the plain lines the numerical results. As can be seen, the numerical shrinkage is very close to the experimental in both direction which was made possible using an orthotropic mechanical law. A ratio $\frac{E_{//}}{E_{\perp}} = 2$ is used which is in accordance with studies on the transverse anisotropy of overconsolidated clay [GAR 73] and this range of value was already used for Boom clay in the work of Dizier [DIZ 11].

6. Conclusion

This paper has presented the formulation of a thermo-hydro-mechanical model for the study and analysis of the drying behavior of Boom clay samples. The main focus of this study was to validate the capacity of the model to closely reproduce experimental behavior. First, the experimental campaign used as validation was introduced [PRI 16]. Then, the different sub-model were thoroughly presented. The hydraulic model is based on Richard's equation for water flow in unsaturated soils using van Genuchten's formulation to determine the saturation degree and relative permeability. The thermal model is a classical energy balance equation. The mechanical model is an orthotropic elastic model expressed in Bishop's effective stress.

Finally, numerical simulations were conducted in order to show the performance of the proposed model. The simulation results showed that the model is capable of closely reproducing the observed behavior.

Going forward, there are still a few improvements that could be brought into the proposed model. One of them is to consider the cracking that may occur during the drying process and its effect on the drying kinetics. Since Boom clay presents a clear bedding, if cracking occurs, it will be alongside the bedding planes being a "weakness" in the medium structure. To represent that behavior, a suggested lead is to use interface finite elements to reproduce crack propagation and use experimental data to validate it.

7. Bibliographie

[Bel 13] BELGIUM PROFILE, Radioactive waste management programmes in OECD/NEA member countries, rapport, Nuclear energy agency, 2013.

- [BER 07] BERNIER F., LI X. L., BASTIAENS W., « Twenty-five years' geotechnical observation and testing in the Tertiary Boom Clay formation », *Géotechnique*, vol. 57, n° 2, p. 229–237, Thomas Telford Ltd, 2007.
- [BLÜ 07] BLÜMLING P., BERNIER F., LEBON P., MARTIN C. D., « The excavation damaged zone in clay formations time-dependent behaviour and influence on performance assessment », *Physics and Chemistry of the Earth, Parts A/B/C*, vol. 32, n° 8, p. 588–599, Elsevier, 2007.
- [CHE 11] CHEN G., SILLEN X., VERSTRICHT J., LI X. L., « ATLAS III in situ heating test in boom clay : Field data, observation and interpretation », *Computers and Geotechnics*, vol. 38, n° 5, p. 683–696, Elsevier, 2011.
- [CRA 09] CRAEYE B., DE SCHUTTER G., VAN HUMBEECK H., VAN COTTHEM A., « Early age behaviour of concrete supercontainers for radioactive waste disposal », *Nuclear Engineering and Design*, vol. 239, n° 1, p. 23–35, Elsevier, 2009.
- [DEH 05] DEHANDSCHUTTER B., VANDYCKE S., SINTUBIN M., VANDENBERGHE N., WOUTERS L., « Brittle fractures and ductile shear bands in argillaceous sediments : inferences from Oligocene Boom Clay (Belgium) », *Journal of Structural Geology*, vol. 27, n° 6, p. 1095–1112, Elsevier, 2005.
- [DIZ 11] DIZIER A., Caractérisation des effets de température dans la zone endommagée autour de tunnels de stockage de déchets nucléaires dans des roches argileuses, PhD thesis, Université de Liège (Belgique), 2011.
- [GAR 73] GARNIER J., Tassement et contraintes : influence de la rigidité de la fondation et de l'anisotropie du massif, PhD thesis, 1973.
- [GER 08] GERARD P., CHARLIER R., CHAMBON R., COLLIN F., « Influence of evaporation and seepage on the convergence of a ventilated cavity », *Water resources research*, vol. 44, n° 5, Wiley Online Library, 2008.
- [GER 10] GERARD P., LÉONARD A., MASEKANYA J.-P., CHARLIER R., COLLIN F., « Study of the soil-atmosphere moisture exchanges through convective drying tests in non-isothermal conditions », *International journal for numerical and analytical methods in geomechanics*, vol. 34, n° 12, p. 1297–1320, Wiley Online Library, 2010.
- [HOR 87] HORSEMAN S., WINTER M., ENWISTLE D., Geotechnical characterization of Boom clay in relation to the disposal of radioactive waste, rapport, Commission of the European Communities, 1987.
- [IDS 74] IDSO S., REGINATO R., JACKSON R., KIMBALL B., NAKAYAMA F., « The three stages of drying of a field soil », *Soil Science Society of America Journal*, vol. 38, n° 5, p. 831–837, Soil Science Society of America, 1974.
- [IEA 03] IEAA, Scientific and Technical Basis for the Geological Disposal of Radioactive Wastes, rapport, International Atomic Energy Agency, Viena, 2003.
- [KOW 12] KOWALSKI S. J., *Thermomechanics of drying processes*, vol. 8, Springer Science & Business Media, 2012.
- [LAN 88] LANCZOS C., *Applied analysis*, Courier Corporation, 1988.
- [LEO 02a] LÉONARD A., Étude du séchage convectif des boues de station d'épuration - Suivi de la texture par microtomographie à rayon X, PhD thesis, Université de Liège (Belgique), 2002.
- [LÉO 02b] LÉONARD A., BLACHER S., MARCHOT P., CRINE M., « Use of X-ray microtomography to follow the convective heat drying of wastewater sludges », *Drying Technology*, vol. 20, n° 4-5, p. 1053–1069, Taylor & Francis, 2002.
- [LÉO 05] LÉONARD A., BLACHER S., MARCHOT P., PIRARD J.-P., CRINE M., « Convective drying of wastewater sludges : Influence of air temperature, superficial velocity, and humidity on the kinetics », *Drying technology*, vol. 23, n° 8, p. 1667–1679, Taylor & Francis, 2005.
- [MUS 07] MUSIELAK G., JACEK B., « Non-linear heat and mass transfer during convective drying of kaolin cylinder under non-steady conditions », *Transport in porous media*, vol. 66, n° 1-2, p. 121–134, Springer, 2007.
- [NAD 95] NADEAU J.-P., PUIGGALI J.-R., « Séchage : des processus physiques aux procédés industriels », Paris (France) Technique et Documentation-Lavoisier, 1995.
- [NEA 08] NEA, Moving Forward with Geological Disposal of Radioactive Waste, A Collective Statement by the NEA Radioactive Waste Management Committee (RWMC), rapport, OECD-Nuclear Energy Agency, Paris, 2008.
- [OND 01] ONDRAF/NIRAS, Technical overview of the safir 2 report : Safety assessment and feasibility interim report 2, rapport, 2001.
- [PRI 16] PRIME N., LEVASSEUR S., MINY L., CHARLIER R., LÉONARD A., COLLIN F., « Drying-induced shrinkage of Boom clay : an experimental investigation », *Canadian Geotechnical Journal*, vol. 52, n° 999, p. 1–14, NRC Research Press, 2016.
- [VAN 80] VAN GENUCHTEN M. T., « A closed-form equation for predicting the hydraulic conductivity of unsaturated soils », *Soil science society of America journal*, vol. 44, n° 5, p. 892–898, Soil Science Society of America, 1980.
- [WEM 08] WEMAERE I., MARIVOET J., LABAT S., « Hydraulic conductivity variability of the Boom Clay in north-east Belgium based on four core drilled boreholes », *Physics and Chemistry of the Earth, Parts A/B/C*, vol. 33, p. S24–S36, Elsevier, 2008.